Open Archive Toulouse Archive Ouverte

OATAO is an open access repository that collects the work of Toulouse researchers and makes it freely available over the web where possible

This is an author's version published in: https://oatao.univ-toulouse.fr/26042

Official URL:

https://doi.org/10.1109/TPS.2020.2985406

Any correspondence concerning this service should be sent to the repository administrator: tech-oatao@listes-diff.inp-toulouse.fr

Low voltage plasma jet with piezoelectric generator : preliminary evaluation of decontamination capabilities

Jordan Stekke, Claire Tendero, Pascal Tierce, Christian Courtois, Gaetan Rauwel, Juslan Lo, Philippe Guillot, Francois Pigache

Abstract— **This paper deals with the proof of concept and the preliminary evaluation of decontamination performances obtained with a plasma jet generated by a piezoelectric transformer. This low voltage supply solution (<10V) is investigated as a plasma jet device, compact and safe solution for the decontamination of medical thermo-sensitive devices. The principle of the piezoelectric generator is presented, followed by the optical spectroscopy of the plasma jet, the protocol conditions for the bactericidal effect observations and finally the reduction rates obtained on Pseudomonas aeruginosa and Staphylococcus aureus bacteria strains with an argon plasma jet at atmospheric pressure about 2.5W electrical input power.**

Index Terms: piezoelectric transformer; atmospheric plasma jet; decontamination

I. INTRODUCTION

Historically the studies on plasma for biomedical issues started focusing on the disinfection capabilities of low temperature plasma in the early 90's [1-4]. Thanks to the wide range of plasma interactions with living cells, the recent research directions have been oriented towards therapy considerations [5-6]. Numerous plasma generators have been developed to satisfy the disinfection requirements of thermo-sensitive or chemo-sensitive tools. Some examples of plasma jet (or needles) solutions for different applications are briefly described in Table 1. Many difficulties such as a high disinfection level (particularly on high aspect ratio parts), a minimal duration of treatment, still have to be overcome [7].

TABLE 1: EXAMPLES OF PLASMA JET SOURCES

Application field	Operating conditions	Target / issue
Oncology	Pulsed RF source 1.2 kV RMS / 3 W Gas flow: 3 slm , 98% Ne / 2% Ar	Melanoma cells (in vitro & in vivo tests) [8]
Dentistry	2.6 kHz 1.1 W Air	E. Faecalis [9]
Desinfection	27.12MHz RF source 20 W Gas flow: 20 slm Ar	B. Atrophaeus E. coli [10]
	4-6kV pulsed source 100ns pulse width 2kHz repetition Gas flow: 5 slm, He / 1% O_2	B. Atrophaeus [11]
Wound healing	Array of μplasma jets 20 kHz 1 kV RMS Gas flow: 1.5 slm, He	2nd degree burns [12]
	kINPen (neoplastools) 1MHz 1 kV / 3.5 W Gas flow: 3 slm, Ar	Chronic wounds on domestic animals, clinical observations on leg ulcers [13]
Risk assessment	kINPen	Genotoxicity and mutagenic potential of argon plasma [14]
	25 kHz 3 kV / 2mA Gas flow: A few slm, He	Skin damage on mouse [15]

Although these different sources operate at various frequencies ranging from kHz up to MHz with different DBD designs (most of the time a metal needle inserted in a quartz tube), they all require a high voltage source as input in order to initiate and sustain the discharge (depending on the gas, flow, dielectric configurations…). In some applications and depending on the required output power, such high voltage generators can be inappropriate. The proposed technology in this paper may be an alternative.

II. DESCRIPTION OF THE PLASMA SOURCE

A. Principle of a piezoelectric plasma generator

This section briefly introduces the piezoelectric properties and then focuses on the use of a piezoelectric transformer device for plasma discharge. The piezoelectric property is the ability of some (mono or poly crystalline) materials to develop an electric potential when they undergo a mechanical stress [16-17]. Moreover this property is reversible.

The research on this topic really started in 2000's leading to a significant understanding of this technology [18-19]. Since then, the piezoelectric transformer as plasma generator has been explored in various applications such as an ozonizer [20], an excimer lamp VUV light source [21], an ignitor for pulsed plasma thrusters [22], a micro-thruster for satellite positioning control [23], an ionic wind source [24], a source for deuterium or hydrogen neutron production [25], or a patented source for ambient mass spectrometry at atmospheric pressure [26].

The first patent of piezoelectric transformer appears in 1931, explaining the concept [27]. More than 20 years later, in 1954, C.A. Rosen et al. have described some designs which are still used at the present time [28]. The piezoelectric technology is particularly suitable for compact devices as demonstrated by their use in micro-sensors and micro-actuators. Most of piezoelectric transformers are made with hard PZT ceramic (Lead Zirconate Titanate). The maximal power density of such hard piezoceramic can be estimated to 300W/cm³ [29] which suggests a wide range of possibilities. Nevertheless, it is also bounded by a set of technical limitations;
- The Curie temperature limitation. Over this limit (which could be around 200°C depending on the ceramic composition), the remanent polarization vanishes and consequently the piezoelectric capability as well,
- The mechanical break of the ceramic, induced by excessive mechanical stress.

The principle of the piezoelectric transformer relies on the association of two (or more) piezoelectric elements that are mechanically coupled. The first is excited by an external alternative electric supply applied by electrodes, resulting in mechanical vibrations (the reverse piezoelectric effect). This latter is qualified as the primary side, later referred to as "primary". The second element also vibrates, inducing an electric field (direct piezoelectric effect) and it is qualified as the secondary side. Thus, the operation relies on two successive electromechanical conversions, enabling a voltage/current adaptation, an impedance adaptation, a high insulation level. Since this conversion results from the conversion of mechanical energy (propagating vibrations), the performances of such a component are strongly dependent on the geometry, the operating frequency, the electrode distribution and the piezoelectric material properties. Significant description and modelling of piezoelectric transformer designs and particularities are further discussed in literature [31-32]. For optimal efficiency and a maximum output voltage, piezo-transformers should be supplied at an operating frequency close to a resonant frequency of the structure. When the primary side is supplied close to one of the longitudinal resonant modes, a standing wave vibration occurs in the material and an electric potential distribution is obtained on secondary.

In the frame of plasma generation, the most interesting architectures are the high step-up voltage transformers: they can reach a voltage gain higher than 100 giving the opportunity to design a compact generator supplied with a very low input voltage.

The present piezo plasma generator uses a classical so-called Rosen-type transformer as illustrated in Fig. 1.
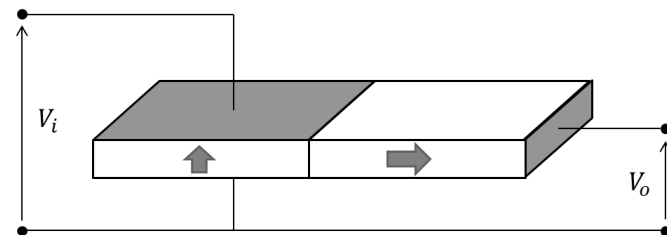

Fig. 1 Design of the step-up Rosen type transformer [30].

The various dimensions and material properties of the Rosen type transformer used in this study are summarized in Table 2.

TABLE 2: PIEZO TRANSFORMERS CHARACTERISTICS

ceramic	Hard PZT
total length	30.4 mm
width	7.6 mm
thickness	2.3 mm
operational vibratory mode	$\lambda/2$
operating frequency	~53kHz
relative permittivity in poling axis at constant stress ε_{33}^T	1600
density ρ	7900 kg/m3
transverse compliance at constant $\langle E \rangle$ field s_{11}^E	1.19×10^{-11} m²/N
longitudinal compliance at constant $\langle E \rangle$ field s_{33}^E	1.39×10^{-11} m²/N
transverse piezoelectric coefficient d_{31}	-155×10^{-12} m/N
longitudinal piezoelectric coefficient d_{33}	3640×10^{-12} m/N

For plasma generation, the piezoelectric transformers can be used in two different ways:

■ As a simple two-port step-up voltage component. The electric charges are collected on the secondary side by a metal needle [33], or between two electrodes with a narrow gap and separated by a dielectric layer [34].

■ Another configuration directly involves the secondary surface as a dielectric layer which supports the discharge [35-36]. In such a configuration, there is no need for the secondary electrode. This particular configuration prevents sparks (DBD-like configuration) and it benefits from the high dielectric constant of the material. Let us remember that the relative permittivity of PZT ceramic is about several hundred units ($\varepsilon r \approx 1000$ for hard PZT ceramic). This latter implementation has been selected for this study.

Contrary to a passive dielectric layer in conventional DBD, the electric potential on the piezo surface is not uniform and depends on the excited resonant vibratory mode. Consequently, for the first longitudinal vibratory modes, the theoretical electric potential distribution is illustrated in Fig. 2(a). This distribution drives the plasma discharge location surrounding the transformer surface (Fig. 2(b)). Moreover, the electric potential amplitude is strongly a function of the input voltage supply, the mechanical damping coefficient and the operating angular pulsation. With the appropriate operating conditions this maximum potential value can reach several kV.
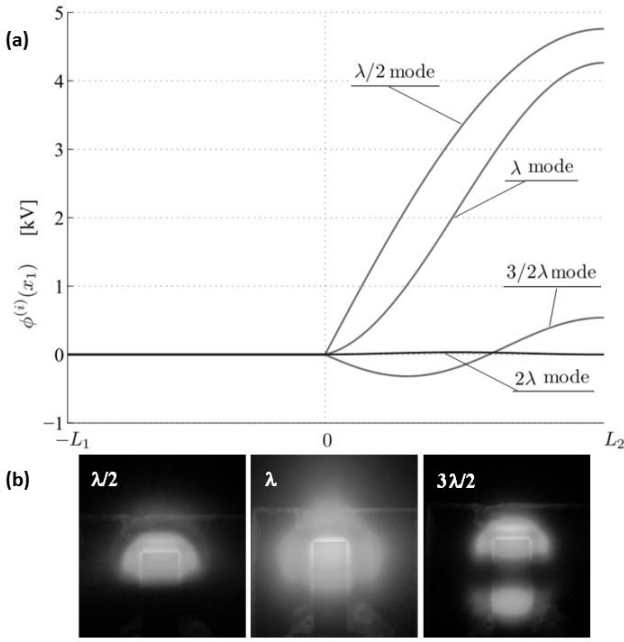
Fig. 2. (a) Theoretical electric potential on the transformer surface for the first four longitudinal vibratory modes. (b) Plasma discharges for first three modes obtained at a pressure of 10mbar in air [37].

The Piezoelectric Transformer (PT) is a resonant device which can be relevantly simulated by an equivalent electrical circuit. This latter is valid in the vicinity of the resonant mode and element values are dependent on the geometry and the material properties.
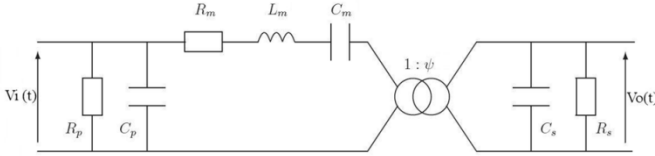

Fig. 3 The electric equivalent circuit of piezo transformer

As emphasized in Fig. 3, the PT is essentially capacitive due to the primary side. Its electrical behavior changes when supplied at its mechanical resonant frequency simulated by the two parameters L_m and C_m. The voltage gain is depicted by factor ψ. The expressions of the equivalent circuit parameters are not given in detail in this paper. However there is a considerable body of research devoted to the modelling [38].

As a consequence of the non-linear behavior of the plasma discharge and the load dependency of the voltage gain, the output voltage on the transformer termination is rather complicated to evaluate. This constitutes the main difference with conventional plasma generators and prevents the direct measurement of the plasma power. In the present case, the experimental output voltage can be evaluated from indirect methods such as laser interferometry. These considerations will be the purpose of future work and the present paper only mentions the electrical measurements from the primary side.

The output voltage of the transformer highly depends on the concordance of the device's supply and the resonant frequencies. Moreover, the resonant frequency tends to slightly shift with the steady state electric load (plasma load) and the transformer temperature rising. As a consequence, a control feedback is essential to track the operating point and to maintain a stable plasma jet. This optimal operating point is maintained by the admittance phase tracking [39]. Then, the used generator requires an input voltage of 2.7Vrms. Even if the streamer plasma regime implies a nonperiodic behavior, the electrical consumption can be evaluated by the measurement of the input current, resulting in an average input power of 2.5W. It must be noticed that this input power does not correspond to the power transmitted to the discharge (due to power losses), nevertheless it informs on the maximum order of magnitude.

For the preliminary bactericidal tests carried out with this piezoelectric technology, an elementary plasma stylus design has been made as illustrated in Fig. 4.
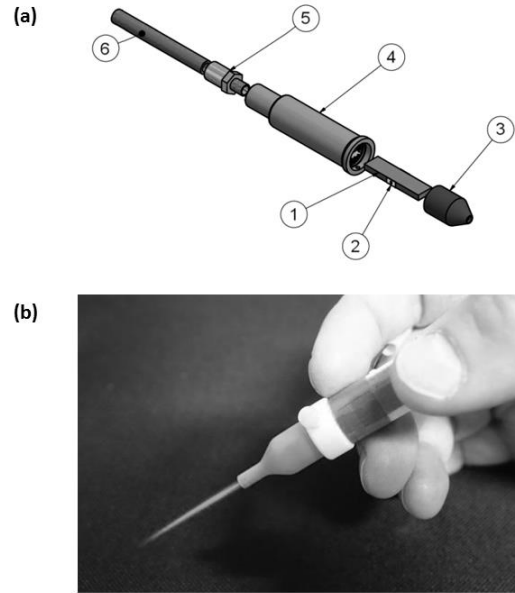

Fig. 4 Design of the piezo-plasma jet stylus (a) : (1) PT (2) electric connectors (3) stylus nozzle (4) stylus body (5) gas connector (6) gas tube. The piezo-plasma jet in operation (b) with a 1slm Ar gas flow

B. Plasma Diagnostics

The characterization of piezo-plasma jet was made by optical emission spectroscopy and by bidimensional emission imaging. An optical spectrometer (HR2000+, Ocean Optics, Grating 1800mm-1, slit 10μm, 200 to 1100nm, maximal optical resolution 0.5nm) coupled to an optical fiber (core diameter 600μm) was used to identify the plasma emission lines [40]. The measurement was realized in order to identify the typical optical emissions of the carrier gas and the reactive species due to the ambient air. The optical fiber was placed perpendicular to the piezo-plasma jet on a micrometric translation stage. Moving the fiber along the piezo-plasma jet, the linear translation system allowed to characterize the axial distribution of the species excited or ionized by the plasma. Moreover, a fast ICCD camera (Princeton PIMAX-2K-RB, 1024x1024) was placed beside the jet, perpendicularly to the source, in order to assess the 2D distribution of plasma emissions within the plasma jet. The jet length was determined from the ICCD

camera data. The experimental setup has been described previously in [40-41].

In the standard operating conditions of the piezo-plasma stylus (1slm Ar gas flow in open air, 1.5Vrms, 53kHz, 2.5W input power), the emission spectra of the discharge were measured. Fig. 5(b) highlights the main emission lines of the plasma jet flowing in air, commonly observed by many authors [38-42] on a reduced wavelength range (300-800nm). Two spectra were recorded in this work. The first one corresponds to the plasma emissions produced inside the source, close to the piezo transformer edge (Fig. 5(a)). The plasma emission is mainly composed by Ar emission lines.

The second one was obtained 15mm away from the stylus outlet (Fig. 5(b)), near the tip of the plasma jet. The UV and visible emissions correspond to the radiative de-excitations of argon, hydroxyl (OH radical) [43], molecular nitrogen and oxygen [44]. The presence of emission lines relative to ambient air species demonstrates the interaction of the plasma jet with its environment. The presence of hydroxyl in the UV-B region (308 nm) is related to processes involving water molecules. The production of the excited nitrogen molecule (second positive system situated in the 300 to 450 nm range) can come from electron collisions from the fundamental as well as from Ar metastable excitation transfer processes to the nitrogen molecules. Oxygen (777 nm) is the last sign of plasma and ambient air interaction [44].
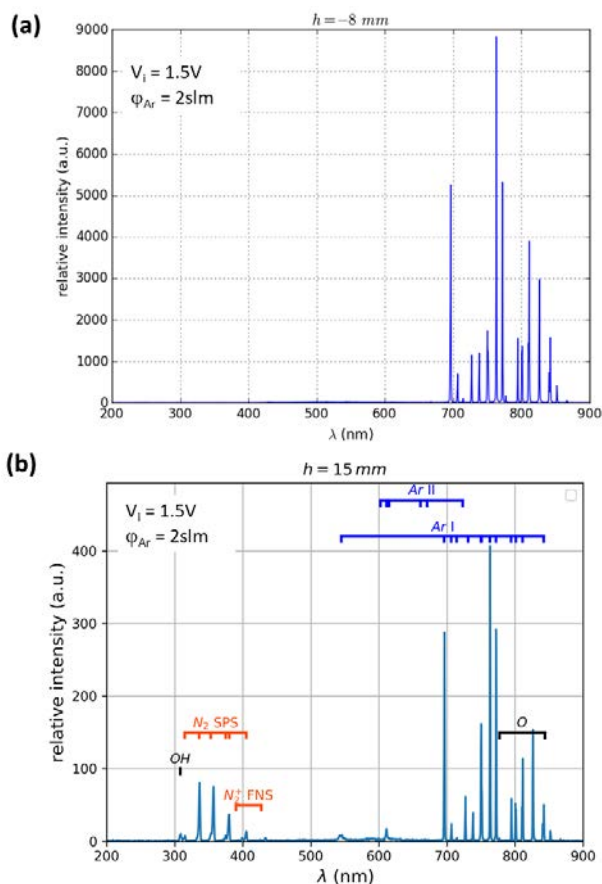

Fig. 5. Main emission lines of the plasma, (a) inside the source, 8 mm before the stylus outlet, and (b) in the plasma jet, 15 mm away from the source outlet.

Additionally, the plasma spatial distribution is measured by fast ICCD camera (Fig. 6). Based on the lines of interest, determined from the emission spectra, two filters that allowed the characterization of species production at the outlet of the nozzle in contact with ambient air have been used. The ICCD camera was also coupled to bandpass interference filters (Thorlabs, 10nm as bandwidth) centered on specific central wavelength values. The first one, centered on 750nm, allowed the assessment of argon distribution. The second one, centered on 380nm, showed the nitrogen distribution.
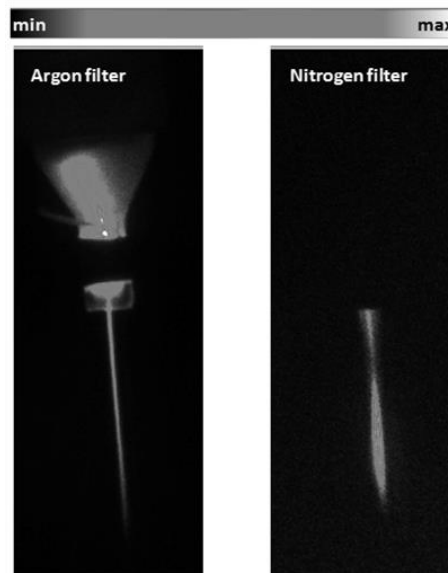

Fig. 6. 2D normalized imaging of the plasma inside and outside the source, 750nm argon filter (left) and 380 nm nitrogen filter (right).

The highest argon emission intensity corresponds to the interior of the source. From the exit of the nozzle, argon emission intensity decreases until plasma extinction at several tens of millimeters distant from the exit. Nitrogen emissions start at the exit of the source. The emission intensity increases, reaches a maximum and then decreases. This maximum emission is located in the intermediate region of the plasma jet. Before this maximum, argon-air ratio is too high and plasma is dominated by argon emissions [46]. After this maximum value is reached, argon-air proportion is too small and the plasma jet is not able anymore to excite ambient air species [45].

III. EXPERIMENTAL SECTION – BACTERICIDAL TEST CONDITIONS

The evaluation of the piezo-plasma jet efficiency used for the first time as a disinfection device is carried out with two different bacteria strains (Gram-positive and Gram-negative):
▪ *Pseudomonas.aeruginosa* - Institut Pasteur - CIP 103 467
▪ *Staphylococcus.aureus* - Institut Pasteur - CIP 4 83
The methodology relies on the adaptation of the EN 13697 protocol (bactericidal effect on non-porous surface). This standard protocol implies operating at ambient temperature (~20°C) and a significant effect is considered when the reduction rate is over 4log compared to the control sample. Each test has been duplicated at least twice to four times to ensure robustness of the experimental results.

The samples are prepared as follow: a 50μL droplet of the initial suspension (that contains between 1.5×10^8 CFU / mL and 5.0×10^8 CFU/ mL of bacteria in tryptone salt diluent) is deposited on a 2cm-diameter stainless steel substrate. Then samples are dried at 37°C in an incubator during 20 minutes before being treated with the plasma jet. It consists in directly and vertically applying the plasma jet on the surface carrying the bacteria inoculum, as illustrated in Fig. 7.
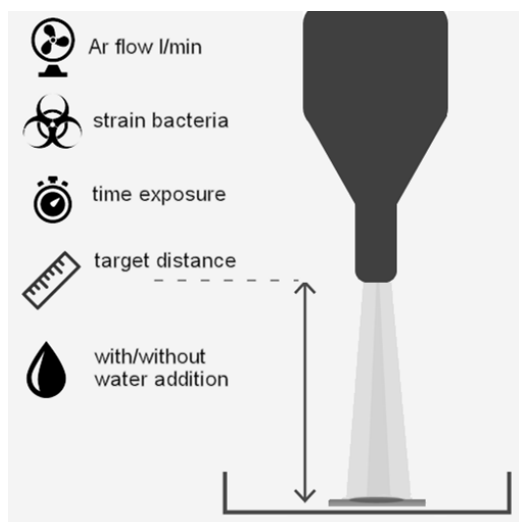

Fig. 7. The plasma jet treatment protocol

After the plasma treatment, the stainless steel samples are transferred into a 10mL container of the tryptone-salt diluent where the microorganisms are removed from the disk by shaking with glass beads. This mixture is 10 to 100 diluted and 1mL is grown in TSA (15ml to 20ml) in an incubator at 36 ° C during 2×24h. Only Petri dishes ranging from 15 up to 300 CFU + -10% are used for counting.

The operating plasma discharge regime is comparable to a glow discharge, obtained by simply placing the plasma jet in contact with the inoculum without any particular layout.

The experimental details of the procedure are presented in Table 3. The log reduction is finally evaluated for different exposure times for both bacteria strains. The authors are aware that several bactericidal actions operate during the exposure period, leading to the slope variation of the log reduction [47]. In this preliminary study, the purpose is to observe if the piezoelectric generator can provide significant bactericidal effect (4 log reduction and beyond) during a sufficient exposure period.

TABLE 3: EXPERIMENTAL CONDITIONS

Bacteria strain	Operating conditions
S. Aureus	• ON / OFF device • without / with 100 μL droplet water • 1.5 cm target distance • Gaz flow rate : ~ 1slm argon
P. Aeruginosa	• Exposure duration: 2, 5, 10, 15, 20 min

Due to the fact that the presence of water in any plasma activated water (PAW) significantly favors the biocidal effect [48-49], tests are carried out in two configurations: dry conditions and with the addition of 100μl-distilled-water

droplet on the inoculum surface. Log reduction on both bacteria strains is presented in Fig. 8.
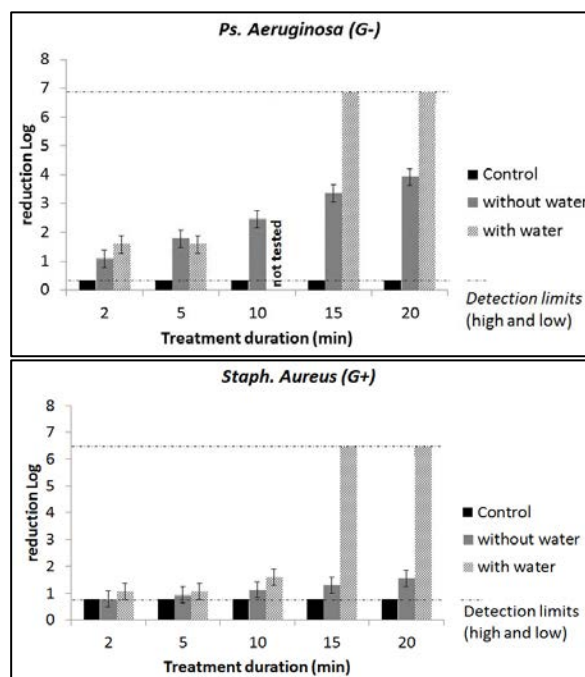

Fig. 8. The log reduction according to the exposure time and operational conditions

IV. RESULTS AND DISCUSSION

C. Bactericidal performances

Several observations can be deduced from results presented in Fig. 8. Firstly, the exposure of the dried inoculum to an argon gas flow without the plasma discharge (control sample) does not result in significant bactericidal effect: whatever the duration of the exposure period, the log reduction does not change in these conditions. On the contrary, after a few minutes exposure period to plasma discharge, log reduction is observable for both bacteria strains. Therefore, the following conclusions can be drawn:

- The longer the exposure time, the higher the reduction of bacteria, which is consistent with any other plasma treatments presented in research.
- As already demonstrated in research the Staphylococcus aureus (gram-positive) is more resistant than the Pseudomonas aeruginosa (gram-negative) [46].
- The presence of water in the decontamination process radically improves the efficiency, including those observed with the S. aureus. After a 15- minutes-exposure, both strains have reached the maximum measurable reduction factor (over 6.73 log). Please note that the droplet water has completely evaporated after 10 minutes of exposure.

In spite of the low input power applied to the piezoelectric device (about 2.5W at 53kHz), the disinfection capacity is clearly visible. Obviously, the exposure time treatment has to be reduced to generate more interest in this technology. The piezoelectric component can be highly improved to be adapted to this new use. However these results are quite promising with regard to the maximum measurable value obtained.

D. The technical limits and improvement perspectives

Even if the piezoelectric technology can bring some advantages in terms of product safety, compactness, low voltage supply, it is also subjected to some technical limits which require attention. Firstly, the electric potential significantly depends on the amplitude vibration produced in the piezo material. The vibration implies mechanical stress in a precise location. All necessary precautions should be taken to prevent brittleness, for example by a specific transformer design or by limiting the mechanical stress during the operation [51]. Moreover, depending on the plasma location and its regime, excessive discharge power density is likely to occur at an unsuitable location of the transformer surface. This can damage the material by erosion and local heating. This phenomenon is observed at the edge of the primary electrode [50]. Such a sparking event can be prevented by depositing a thin coating of a dielectric material on the piezo surface. However this dielectric layer should also be able to withstand the vibration of its substrate. Another solution can be to use other piezoelectric materials more resistant to erosion s(ex: single crystal lithium niobate).

Finally, the piezoelectric property can vanish making the transformer inoperative if its temperature exceeds the Curie temperature: indeed at this temperature a reversible change in the crystalline occurs and results in the depolarization of ferroelectric material. The temperature rise is essentially due to the self-heating induced by the internal friction force. The typical Curie temperature limit is below 250°C for standard PZT hard ceramic.

All these technical precautions actually limit the power of such a piezo plasma generator to a few watts. However, specific design and precautions may enhance the power availability and thus the resulting bactericidal properties. Finally, the modification of the feedgas mixture will also improve the bactericidal effect as widely demonstrated in literature.

V. CONCLUSION

Preliminary decontamination tests have been carried out with an atmospheric pressure plasma jet generated by a piezoelectric transformer. An elementary plasma stylus has been designed with a standard off the shelf transformer, supplied by few volt voltage source. To prevent the frequency discrepancy due to the thermal effect, a simple phase locked loop is added to maintain plasma discharge over time. This plasma jet relies on 1slm argon gas flow and is finally applied to two different bacteria strains following the recommendations of EN 13697 protocol. The resulting reduction rate obtained with this argon plasma jet has reached significant bacteria reduction. This low voltage solution gives rise to the opportunity to develop safe low voltage plasma generators. Nevertheless at this development stage, a specific design of the piezoelectric element is required. This should be associated to an appropriate feedback control and feedgas mixture to significantly improve these promising preliminary results.

REFERENCES

[1] M. Laroussi, "Nonthermal decontamination of biological media by atmospheric-pressure plasmas: Review, analysis and prospects", *IEEE trans. on plasma science*, vol. 30, n 4, pp. 1409-1415, 2002.

[2] M. Laroussi, "Low temperature plasma-based sterilization: Overview and state-of-the-art", *Plasma processes and polymers,* vol. 2, n 5, pp. 391-400, 2005.

[3] M. Laroussi, X. Lu and M. Keidar, "Perspective: The physics, diagnostics and applications of atmospheric pressure low temperature plasma sources used in plasma medicine ", *Journal of Applied Physics,* vol. 122, p. 020901, 2017.

[4] J. Gay-Mimbrera, M. García, B. Isla-Tejera et al , "Clinical and biological principles of cold atmospheric plasma application in skin cancer ", *Advances in Therapy,* vol. 33, n 6, pp. 894-909, 2016.

[5] M. Keidar, D. Yan, I.I. Beilis, B. Trink, J.H. Sherman, "Plasmas for treating cancer: Opportunities for Adaptive and Self-Adaptive Approaches", *Trends in biotechnology*, vol. 36, n 6, pp. 586-593, 2018.

[6] X. Lu, M. Keidar, M. Laroussi, E. Choi, E.J. Szili, K. Ostrikov, "Transcutaneous plasma stress: From soft-matter models to living tissues", *Materials Science and Engineering R Reports*, vol. 138, pp 36-59, 2019.

[7] M. Leggett, G. McDonnell, S. Denyer, P. Setlow and J. Maillard, "Bacterial spore structures and their protective role in biocide resistance" *Journal of applied microbiology,* vol. 113, n 3, pp. 485-498, 2012.

[8] Y. Binenbaum, G. Ben-David, Z. Gil, Y. Slutsker, M. Ryzhkov, J. Felsteiner, Ya. E. Krasik, J. T. Cohen, "Cold atmospheric plasma, created at the tip of an elongated flexible capillary using low electric current, can slow the progression of melanoma", *Plos One,* vol. 12, n 1, p. e0169457, 2017.

[9] Y.-T. Chang and G. Chen, "Oral bacterial inactivation using a novel low-temperature atmospheric-pressure plasma device", *Journal of Dental Sciences,* vol. 11, pp. 65-71, 2016.

[10] K. D. Weltmann, R. Brandenburg, T. von Woedtke, J. Ehlbeck, R. Foest, M. Stieber and E. Kindel, "Antimicrobial treatment of heat sensitive products by miniaturized atmospheric pressure plasma jets (APPJs) ", *Journal of physics D applied physics,* vol. 41, n 19, 2008.

[11] C. Jiang, M.-T. Chen and C. Schaudinn, "Pulsed Atmospheric-Pressure Cold Plasma for Endodontic Disinfection", *IEEE trans. on plasma science,* vol. 37 , n 7, pp. 1190-1195, 2008.

[12] O. Lee, H. Ju, G. Khang, P. Sun, J. Riviera, J. H. Cho, S.-J. Park, J. Eden and C. H. Park, "An experimental burn wound-healing study of non-thermal atmospheric pressure microplasma jet arrays", *Journal of Tissue Engineering and Regenerative Medicine,* vol. 10, pp. 348-357, 2016.

[13] S. Bekeschus, A. Schmidt, K. Weltmann and T. von Woedtke, "The plasma jet kINPen - A powerful tool for wound healing", *Clinical Plasma Medicine,* vol. 4, pp. 19-28, 2016.

[14] K. Wende, S. Bekeschus, A. Schmidt, L. Jatsch, S. Hasse, K. Weltmann, K. Masur and T. von Woedtke, "Risk assessment of a cold argon plasma jet in respect to its mutagenicity", *Mutation Research/Genetic toxicology and environmental mutagenesis,* vol. 798-799, pp. 48-54, 2016.

[15] S. Kos, T. Blagus, M. Cemazar, G. Filipic, G. Sersa and U. Cvelbar, "Safety aspects of atmospheric pressure helium plasma jet operation on skin: In vivo study on mouse skin", *PLos one,* vol. 12, n 4, p. e0174966, 2017.

[16] J. Yang, An introduction to the theory of piezoelectricity, S. S. Media, Ed., New-York, 2005.

[17] T. Ikeda, Fundamentals of piezoelectricity, O. U. Press, Ed., New-York, 1996.

[18] H. Itoh, K. Teranishi and S. Suzuki, "Plasma Sources Science and Technology, Discharge plasmas generated by piezoelectric transformers and their applications", *Plasma Sources Science and Technology,* vol. 15, n 2, 24 April 2006.

[19] M. Teschke and J. Engemann, "Piezoelectric low voltage atmospheric pressure plasma sources", *contribution to plasma physics,* vol. 49, n 9, pp. 614-623, 2009.

[20] K. Teranishi, S. Suzuki and H. Itoh, "A novel generation method of dielectric barrier discharge and ozone production using a piezoelectric transformer," *Japanese Journal of Applied Physics,* vol. 43, no. 9B, pp. 6733–6739, 2004.

[21] K. Teranishi and H. Itoh, "A compact excimer lamp constructed by piezoelectric transformer", *J. Light & Visual environment,* vol. 31, n 1, pp. 5-10, 2007.

[22] A. Carazo, "Piezoelectric transformers for space applications", *5th International Conference on Intelligent Materials*, 2003.

[23] B. T. Hutsel, S. D. Kovaleski, E. A. Baxter and J. W. Kwon, "Charged-particle emission and self-biasing of a piezoelectric transformer Plasma source", *IEEE Trans. on Plasma Science,* vol. 41, n 1, pp. 99-105, January 2013.

[24] M. J. Johnson and D. B. Go, "Piezoelectric transformers for low-voltage generation of gas discharges and ionic", *Journal of Applied Physics,* vol. 118, n 243304, pp. 1-10, 2015.

[25] E. A. Baxter, S. D. Kovaleski, B. B. Gall, J. A. VanGordon, P. Norgard and G. E. Dale, "Hydrogen and deuterium ion extraction from a piezoelectric transformer plasma source", *IEEE Trans. Plasma Sci.,* vol. 42, n 10, p. 3253-3257, october 2014.

[26] E. L. Neidholdt and J. L. Beauchamp, "Switched ferroelectric plasma ionizer", US patent 8,247,784,B2, august 2012.

[27] A. McLean Nicolson, "Piezo electric crystal transformer", U.S. Patent 1 829 234, 27 October 1931.

[28] C.A. Rosen, K.A. Fish and H.C. Rothenberg, "Electromechanical transducer", U.S. Patent 2 830 274, april 1958.

[29] A.M. Flynn and S.R. Sanders, "Fundamental Limits on Energy Transfer and Circuit Considerations for Piezoelectric Transformers", *IEEE trans. on power electronics*, vol. 17, n 1, 2002.

[30] M. Laroussi, C. Tendero, X. Lu et al , "Inactivation of Bacteria by the Plasma Pencil", *Plasma processes and polymers,* vol. 3, n 6-7, pp. 470-473, 2006.

[31] J. Yang, "Piezoelectric transformer structural modeling – a review", *IEEE Trans. Ultrason. Ferroelectr. Freq. Control,* vol. 54, n 6, pp. 1154-1170, June 2007.

[32] J. Erhart, "Bulk piezoelectric ceramic transformers", *Advances in applied ceramics, ,* vol. 112:2, pp. 91-96, 2013.

[33] M. Johnson, D. Boris, T. Petrova and S. Walton, "Characterization of a compact, low-cost atmospheric-pressure plasma jet driven by a piezoelectric transformer", *IEEE Transactions on Plasma Science,* vol. 47, n 1, pp. 1-11, 2018.

[34] I. Kartashev, T. Vontz and H. Florian, "Regimes of piezoelectric transformer operation", *Measurement Science and Technology,* vol. 7, pp. 2150-2158, 2006.

[35] K. Teranishi, S. Suzuki and H. Itoh, "Luminous phenomenon of silent discharge using a piezoelectric transformer", *Jpn. J. Appl. Phys.,* vol. 40, n 9B, p. 5766–5768, september 2001.

[36] H. Itoh, K. Teranishi and S. Suzuki, "Observation of light emissions around a piezoelectric transformer in various gases", *IEEE Trans. Plasma Sci.,* vol. 30, n 1, pp. 124-125, February 2002.

[37] C. Nadal, F. Pigache, Y.Lefèvre, "Analytical modeling of electrical potential repartition on piezoelectric transformer", *2010 IEEE Int. Frequency Control Symposium*, june 2010, NewPort Beach, California.

[38] J. Erhart, P. Pulpan and M. Pustka, "Piezoelectric Ceramic Resonators", *Springer International Publishing AG*, 2017.

[39] M. Kahalerras, F. R. J. Pigache and F. Mosser, "Analyses of temperature influence in piezoelectric transformers dedicated to plasma generation", *IEEE 12th International Workshop of Electronics, Control, Measurement, Signals and their application to Mechatronics (ECMSM)*, Liberec, Czech Republic, 2015.

[40] A. Kone, F. P. Sainct, C. Muja, B. Caillier and P. Guillot, "Investigation of the interaction between a helium plasma jet and conductive (metal)/ non-conductive (dielectric) targets", *Plasma Medicine journal,* vol. 7, n 4, pp. 333-346, 2017.

[41] L. Chauvet, L. Thérèse, B. Caillier and P. Guillot, "Characterization of an asymmetric DBD plasma jet source at atmospheric pressure", *Anal. At. Spectrom.,* vol. 29, pp. 2050-2057, 2014.

[42] S. Pereira, E. Pinto, P. Ribeiro and S. Sério, "Study of a cold atmospheric pressure plasma jet device for indirect treatment of squamous cell carcinoma", *Clinical Plasma Medicine,* vol. 13, pp. 9-14, 2019.

[43] R. Wanga, S. Y., C. Zhang and P. S. T. Yan, "Comparison between helium and argon plasma jets on improving the hydrophilic property of PMMA surface", *Applied Surface Science,* vol. 367, pp. 401-406, 2016.

[44] H. Yi, N. Lu, J. Pan, J. Li, Y. Wu and K. Feng Shang, "Characteristic study of cold atmospheric argon plasma jets with rod-tube/tube high voltage electrode", *Journal of Electrostatics,* vol. 71, pp. 93-101, 2013.

[45] G. Wattieaux, M. Yousfi and N. Merbahi, "Optical emission spectroscopy for quantification of ultraviolet radiations and biocide active species in microwave argon plasma jet at atmospheric pressure", *Spectrochimica Acta Part B,* vol. 89, pp. 66-76, 2013.

[46] A. G. Volkov, K. G. Xu and V. I. Kolobov, "Cold plasma interactions with plants: Morphing and movements of venus flytrap and mimosa pudica induced by argon plasma jet", *Bioelectrochemistry,* vol. 118, pp. 100-105, 2017.

[47] M. M, J. Barbeau, S. Moreau, J. Pelletier, M. Tabrizan and L. Yahia, "Low-temperature sterilization using gas plasmas : a review of the experiments and an analysis of the inactivation mechanisms", *Internal Journal of Pharmaceutic,* vol. 226, pp. 1-21, 2001.

[48] M. Hahnel, T. von Woedtke and K.-D. Weltmann, "Influence of the air humidity on the reduction of bacillus spores in a defined environment at atmospheric pressure using a dielectric barrier surface discharge", *Plasma processes and polymers,* vol. 7, n 3-4, p. 244–249 , 2010.

[49] G. Kamgang-Youbi, J. Herry, T. Meylheuc, J. Brisset, M. Bellon-Fontaine, A. Doubla and M. Naïtali, "Microbial inactivation using plasma-activated water obtained by gliding electric discharges", *letters in applied microbiology,* vol. 48, n 1, pp. 13-18, 2009.

[50] A. Mai-Prochnow, M. Clauson, J. Hong and A. B. Murphy, "Gram positive and gram negative bacteria differ in their sensitivity to cold plasma", *Scientific reports,* vol. 6, n 38610, 2016.

[51] A. L. Benwell, "A high voltage piezoelectric transformer for active interrogation", *phd thesis dissertation*, University of Missouri-Columbia, december 2009.